Atmospheric
Chemistry
and Physics

Modelling studies of HOMs and their contributions to new particle formation and growth: comparison of boreal forest in Finland and a polluted environment in China

Ximeng Qi[1,2,4], Aijun Ding[1,2], Pontus Roldin[3], Zhengning Xu[1,2], Putian Zhou[4], Nina Sarnela[4], Wei Nie[1,2], Xin Huang[1,2], Anton Rusanen[4], Mikael Ehn[4], Matti P. Rissanen[4], Tuukka Petäjä[4,1], Markku Kulmala[4], and Michael Boy[4]

[1]Joint International Research Laboratory of Atmospheric and Earth System Sciences, School of Atmospheric Sciences, Nanjing University, Nanjing, 210023, China
[2]Collaborative Innovation Center of Climate Change, Nanjing, 210023, China
[3]Division of Nuclear Physics, Lund University, P.O. Box 118, 22100 Lund, Sweden
[4]Institute for Atmospheric and Earth System Research/Physics, Faculty of Science, University of Helsinki, P.O. Box 64, 00014 University of Helsinki, Helsinki, Finland

Correspondence: Aijun Ding (dingaj@nju.edu.cn)

Abstract. Highly oxygenated multifunctional compounds (HOMs) play a key role in new particle formation (NPF), but their quantitative roles in different environments of the globe have not been well studied yet. Frequent NPF events were observed at two "flagship" stations under different environmental conditions, i.e. a remote boreal forest site (SMEAR II) in Finland and a suburban site (SORPES) in polluted eastern China. The averaged formation rate of 6 nm particles and the growth rate of 6–30 nm particles were $0.3\,\mathrm{cm^{-3}\,s^{-1}}$ and $4.5\,\mathrm{nm\,h^{-1}}$ at SMEAR II compared to $2.3\,\mathrm{cm^{-3}\,s^{-1}}$ and $8.7\,\mathrm{nm\,h^{-1}}$ at SORPES, respectively. To explore the differences of NPF at the two stations, the HOM concentrations and NPF events at two sites were simulated with the MALTE-BOX model, and their roles in NPF and particle growth in the two distinctly different environments are discussed. The model provides an acceptable agreement between the simulated and measured concentrations of sulfuric acid and HOMs at SMEAR II. The sulfuric acid and HOM organonitrate concentrations are significantly higher but other HOM monomers and dimers from monoterpene oxidation are lower at SORPES compared to SMEAR II. The model simulates the NPF events at SMEAR II with a good agreement but underestimates the growth of new particles at SORPES, indicating a dominant role of anthropogenic processes in the polluted environment. HOMs from monoterpene oxidation dominate the growth of ultrafine particles at SMEAR II while sulfuric acid and HOMs from aromatics oxidation play a more important role in particle growth. This study highlights the distinct roles of sulfuric acid and HOMs in NPF and particle growth in different environmental conditions and suggests the need for molecular-scale measurements in improving the understanding of NPF mechanisms in polluted areas like eastern China.

1 Introduction

New particle formation (NPF), including the production of molecular clusters and the subsequent growth of these clusters (Kulmala et al., 2014), is a global phenomenon and has been observed under different environmental conditions (Kulmala and Kerminen, 2008; Kulmala et al., 2004; Zhang et al., 2012).). NPF can influence climate by contributing up to 50 % of cloud condensation nuclei (CCN) (Merikanto et al., 2009; Sihto et al., 2011) and can have strong effects on air quality (Shen et al., 2011; Yu et al., 2010; Guo et al., 2014).

Sulfuric acid has been commonly considered one of the main gas precursors of NPF (Kulmala and Kerminen, 2008;

Zhang et al., 2012). Recently, it was found that highly oxygenated multifunctional compounds (HOMs) can participate in the initial steps of NPF by stabilizing sulfuric acid (Schobesberger et al., 2013; Riccobono et al., 2014; Kulmala et al., 2013). Most of the HOM dimers and the most oxidized monomers can be extremely low-volatility organic compounds (ELVOCs) (Kurtén et al., 2016) and most likely contribute to the initial growth of newly formed particles (Trostl et al., 2016). Ehn et al. (2014) showed that monoterpene oxidation is a strong source of HOMs and these HOMs can explain the majority of the observed particle growth from 2 nm up to 50 nm in boreal forest. Recent studies (Jokinen et al., 2015; Trostl et al., 2016) showed that HOMs can enhance atmospheric NPF and growth in most continental regions and increase the CCN concentrations by applying a constant monoterpene HOM yield (achieved from measurement) in a global model. Based on the HOM formation theory described by Ehn et al. (2014), a detailed HOM formation mechanism was applied (Öström et al., 2017).

Currently, the role of HOMs in NPF has been mainly studied in specific environment conditions with intensive observations available, such as the SMEAR II station in a Nordic boreal forest (Yan et al., 2016; Dal Maso et al., 2005). However, understanding the mechanisms of NPF is particularly important from the perspective of air quality. As one of the most economically invigorating and densely populated countries, China has measured NPF events since the last decade (Shen et al., 2011; Wu et al., 2007; Wang et al., 2017; Kivekas et al., 2009). Interestingly, the NPF events were observed frequently in heavily polluted environments in China (Kulmala et al., 2017; Wang et al., 2017). However, no measurements of HOMs in China have been reported until now and the understanding of the roles of HOMs in NPF is very limited. The SORPES station at Nanjing is one of the "flagship" stations in the domain of the Pan-Eurasian Experiment (PEEX) (Kulmala et al., 2015; Lappalainen et al., 2016), providing a completely different environment in comparison to the remote boreal forest.

In this study, the NPF events at SMEAR II and SORPES, including the formation rates, growth rates, and environmental conditions, were compared first. Then, by using the new version of the MALTE-BOX model, the precursor vapour gases (i.e. sulfuric acid and HOMs) and NPF at two sites were simulated to deeply investigate the differences in NPF. This modelling study will increase our understanding of NPF at an urban site in China and examines whether the nucleation and HOM formation mechanisms, which are intensively investigated at SMEAR II in Finland, can be used in a polluted environment in China. In addition, applying a process model like MALTE-BOX, to simulate HOM concentrations and their contribution to the growth of newly formed particles at the two selected sites with different environmental conditions, can validate whether a single HOM formation and nucleation mechanism could be appropriate in global models.

2 Materials and methods

2.1 Site and observation descriptions

SMEAR II station (Station for Measuring Forest Ecosystem–Atmosphere Relations) is located in Hyytiälä, Finland (Fig. 1). The station is a boreal forest site, which is surrounded by a Scots pine forest with high monoterpene emissions. The SORPES station (Station for Observing Regional Processes of the Earth System) is located in Nanjing, eastern China (Fig. 1) (Ding et al., 2013, 2016). The station is a suburban site and about 20 km northeast of downtown Nanjing. The aerosol number size distributions were measured continuously with a differential mobility particle sizer (DMPS) for the size range of 3–1000 nm at SMEAR II and 6–800 nm at SORPES. The trace gases, including O_3, SO_2, and NO_x (NO and NO_2), were measured with online analyzers (Thermo Fisher Scientific 49i, 43i, and 42i, respectively) at both sites. The meteorological parameters, e.g. air temperature, relative humidity, and global radiation, were measured with standard meteorological sensors. Volatile organic compounds (VOCs) were observed using proton-transfer-reaction mass spectrometry (PTR-MS) at SMEAR II continuously at different altitudes. The HOM monomers (molecules with even mass in 300–450 Th), dimers (molecules with even mass in 452–620 Th), organonitrate (represented by seven major molecules, i.e. $C_7H_9O_8NNO_3^-$, $C_{10}H_{15}O_{6-11}NNO_3^-$), and sulfuric acid concentrations were measured at SMEAR II with a chemical ionization atmospheric-pressure-interface time-of-flight mass spectrometer (CI-APi-TOF) (Jokinen et al., 2012) during spring 2013. At SORPES, VOCs were observed with gas chromatography–mass spectrometry (GC-MS) from September to October in 2014 (Xu et al., 2017). A summary of the observations at the two stations used in this study is provided in Table S1 in the Supplement. More details about the two stations and measurements are described by Hari et al. (2013) and Ding et al. (2016).

2.2 Model descriptions

In this study we applied the MALTE-BOX model (the model to predict new aerosol formation in the lower troposphere), a zero-dimensional model, which includes several modules for the simulations of chemical and aerosol dynamical processes (Boy et al., 2006). This model has been successfully utilized in NPF analysis – for instance, reproducing OH radical and gaseous sulfuric acid levels (Petäjä et al., 2009), validating various plausible nucleation mechanisms and particle growth (Boy et al., 2007; S. Wang et al., 2013), and identifying important factors influencing NPF occurrence (Boy et al., 2006, 2008; Ortega et al., 2012).

The gas-phase chemistry was simulated using the Master Chemical Mechanism version 3.3.1 (MCMv3.3.1, http://mcm.leeds.ac.uk/MCM/, last access: 1 August 2018) solved by Kinetic PreProcessor (KPP) (Damian et al., 2002; Jenkin
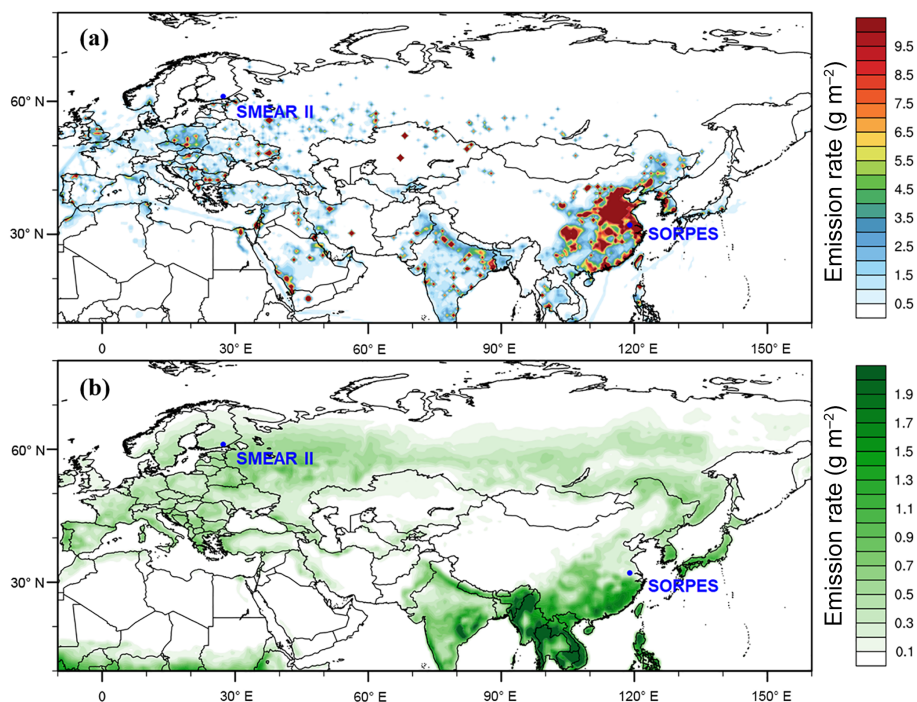
Figure 1. Site (SMEAR II and SORPES) locations on a map of the emission inventory of **(a)** SO_2 and **(b)** monoterpenes (Sindelarova et al., 2014; Granier et al., 2011) (emission inventory data are available at http://eccad.aeris-data.fr, last access: 1 August 2018).

et al., 2003; Saunders et al., 2003). In addition, a new HOM autoxidation mechanism, which is constructed based on the oxidation of monoterpenes (Ehn et al., 2014), was added to MCM v3.3.1. This HOM mechanism explicitly describes the HOM formation processes, i.e. ozone oxidation of monoterpenes, intramolecular H shift, and O_2 additions (autoxidation) (Öström et al., 2017). Moreover, based on Molteni et al. (2016), a simplified mechanism of HOM formation from the oxidation of aromatics by OH was added to MCM v3.3.1. The aerosol dynamical processes were simulated with the size-segregated aerosol model, UHMA (University of Helsinki Multicomponent Aerosol model) (Korhonen et al., 2004). A fixed sectional approach with 120 bins from 1 nm to 2.5 µm in diameter was used. For the smallest size bin, the formation rates of newly formed particles were estimated with the function of sulfuric acid and a first-generation oxidation product of the included monoterpenes, i.e. $J_1 = k \times [H_2SO_4][HOM_{nuc}]$, where HOM_{nuc} was formed with a molar yield of 10^{-5} for each monoterpene reacted with OH (Roldin et al., 2015). The kinetic coefficient (k value) was set for each case to achieve the highest correlation compared to the measured newly formed particles. Organic compounds with pure liquid saturation vapour pressure less than 0.01 Pa were chosen as condensing vapours in UHMA. The saturation vapour pressures of organic compounds in MCM v3.3.1 were estimated with the group contribution method by Nannoolal et al. (2008) using the UMan-SysProp online system (Topping et al., 2016). The satura-

tion vapour pressures of HOMs were calculated using SIM-POL (Pankow and Asher, 2008) as the method of Nanoolal et al. (2008) produces unrealistic estimates of vapour pressures for multifunctional HOMs containing hydroperoxide or a peroxy acid group (Kurtèin et al., 2016). H_2SO_4 was treated as a non-volatile condensing vapour, which generally is a reasonable assumption at typical atmospheric relative humidity and NH_3 levels (Tsagkogeorgas et al., 2017). The coagulation process, dry deposition process, and the dilution of aerosol number concentration caused by boundary layer evolution were estimated in the model as well. Further details about the MALTE model can be found in Sect. S2 in the Supplement.

The measurement variables, i.e. meteorological conditions (e.g. air temperature, relative humidity, pressure, and radiation), trace gases concentrations (e.g. SO_2, O_3, NO, NO_2, CO), and VOCs (e.g. ethylene, ethane, propane, acetone, methyl vinyl ketone, *n*-Butane, benzene, toluene, *o*-/*m*-xylene, 1,2,3/1,2,4-trimethylbenzene, ethylbenzene, isoprene, and monoterpenes), were input into the MALTE-BOX model every 10 min. As monoterpenes were not measured with GC-MS at SORPES, monoterpene concentrations at SORPES were simulated using WRF-Chem, following the method of Huang et al. (2016), in which it was shown that the MALTE-BOX model worked well in NPF simulation with WRF-Chem output of VOCs. The measured aerosol number size distribution was read into the model during the first 5 h. The chemistry scheme was run with a spin-up time of 24 h in

order to achieve a realistic gas-phase composition before the aerosol module was switched on.

3 Results

3.1 Comparisons of NPF at SMEAR II and SORPES

According to long-term observations, the frequency of NPF at SMEAR II is 23 %, with the highest value in spring months (about 40–50 %) (Nieminen et al., 2014). Although the concentration of pre-exiting particles is high, which inhibits NPF, the NPF occurs even more frequently in Chinese megacities such as Nanjing. The frequency of NPF at SOR-PES is 44 %, with the highest value also in spring (55 %) (Qi et al., 2015). As shown in Table 1, the averaged formation rate of 6 nm particles (J_6) at SMEAR II is $0.3 \, \text{cm}^{-3} \, \text{s}^{-1}$ while the J_6 at SORPES is $2.3 \, \text{cm}^{-3} \, \text{s}^{-1}$ on average, which is almost 7 times higher than at SMEAR II. The growth rate of 6–30 nm particles is also higher at SORPES, with $4.5 \, \text{nm} \, \text{h}^{-1}$ at SMEAR II compared to $8.7 \, \text{nm} \, \text{h}^{-1}$ at SORPES on average.

The environmental conditions during NPF at the two sites are substantially different. First, the pre-existing particle loading is much higher at SORPES than at SMEAR II. The condensation sink (CS) at SORPES is almost 20 times higher than at SMEAR II (Table 1). High CS tends to inhibit the occurrence of NPF because of the scavenging of cluster and the loss of gas-phase low-volatility compounds (Kulmala et al., 2017). Second, the concentrations of atmospheric oxidant such as ozone are higher at SORPES (Table 1). Moreover, the concentrations of OH and NO_3 radicals in the Yangtze River Delta urban area of China are higher than in the clean area (S. Wang et al., 2013; Nan et al., 2017). Third, the concentrations of anthropogenic pollutants and biogenic VOCs are distinctly different at the two stations. As an important gas precursor of NPF, the SO_2 concentration at SORPES is almost 50 times higher than at SMEAR II (Table 1). The concentration of NO_x, which is believed to suppress NPF by reacting with peroxy radicals (Wildt et al., 2014), is also much higher at SORPES. The concentrations of anthropogenic volatile organic compounds (AVOCs) are much higher at SORPES while the biogenic volatile organic compound (BVOC) concentrations (e.g. monoterpene and isoprene) are higher at SMEAR II (Hakola et al., 2012; Xu et al., 2017). Given such high anthropogenic VOCs at SORPES, anthropogenic secondary organic aerosol (SOA) is one of the most important SOAs in a polluted area like SORPES (Hu et al., 2017). As the BVOC emissions are quite high in southern China (Fig. 1b), biogenic SOA formation might also be important at SORPES through the interactions between biogenic and anthropogenic emissions, especially when the air masses are from southern China under specific synoptic weather (Zhang et al., 2017, 2016; Carlton et al., 2009). In addition, the meteorological parameters during NPF at the two sites are also
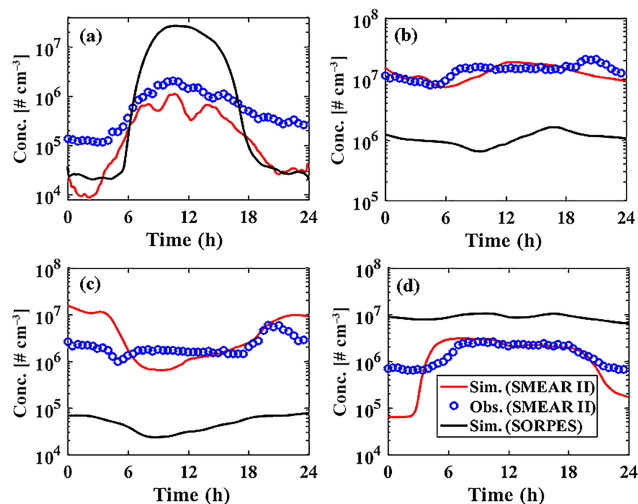

Figure 2. Averaged simulated and measured diurnal cycles of (a) H_2SO_4, (b) HOM non-nitrate monomers, (c) HOM dimers, and (d) HOM organonitrates at SMEAR II and SORPES.

different. Based on the statistics of 1 year of data provided in Table 1, the global radiation and temperature are higher and relatively humidity is lower at SORPES than at SMEAR II during the NPF events.

To study the differences in NPF at SMEAR II and SOR-PES in depth, the 4 NPF days and 1 non-NPF day at each site were chosen for simulations with MALTE-BOX (Table 2). In addition to the differences of NPF parameters and environmental conditions at the two sites described above, monoterpene and benzene concentrations on each day at the two sites are tabulated in Table 2. Because of the high monoterpene emissions in southern China (Fig. 1), the monoterpene concentrations are relatively high at SORPES, especially when the air masses originate from the south. The averaged monoterpene concentration on the chosen days is 0.05 ppbv at SORPES compared to 0.13 ppbv at SMEAR II. The anthropogenic VOCs (e.g. benzene, Table 2) are higher at SOR-PES, as a suburban site, than at SMEAR II, with 0.54 ppbv of benzene concentration at SORPES compared to 0.06 ppbv at SMEAR II on average. The averaged concentration of aromatics (including benzene, toluene, o-/m-xylene, 1,2,3/1,2,4-trimethylbenzene, ethylbenzene) at SORPES on the chosen days was 1.2 ppbv.

3.2 The differences in simulated condensing vapours at two sites

As shown in Fig. 2a, similar to previous studies (e.g. Zhou et al., 2014), the model underestimates the concentrations of sulfuric acid at SMEAR II especially at night. The reasons for this discrepancy could be that there are oxidants other than OH, and Criegee intermediate radicals lead to the formation of sulfuric acid (Boy et al., 2013). Because of the detection limit of the CI-APi-TOF, the HOM non-nitrate

Table 1. Statistics of observed formation rates of 6 nm particles (J_6), growth rates of 6–30 nm particles (GR), condensation sinks (CS), O_3, SO_2 and NO_x concentrations, radiation (Rad.), air temperature (Temp.), and relative humidity (RH) from 09:00 to 15:00 LT on NPF days at SMEAR II and SORPES. Note the statistical samples are the whole-year database of 2013 at SMEAR II and the whole-year database of 2014 at SORPES.

	SMEAR II				SORPES			
	Average	Median	25th	75th	Average	Median	25th	75th
J_6 (cm^{-3} s^{-1})	0.3	0.1	0.06	0.3	2.3	1.6	1	3.5
GR (nm h^{-1})	4.5	2.8	2.0	5.6	8.7	8.0	6.5	10.4
CS (10^{-2} s^{-1})	0.18	0.14	0.08	0.24	3.0	2.7	2.1	3.6
O_3 (ppbv)	36.1	36.6	29.6	41.8	44.7	43.3	28.0	59.1
SO_2 (ppbv)	0.2	0.1	0.03	0.3	9.4	8.0	4.4	12.7
NO_x (ppbv)	0.5	0.2	0.06	0.6	17.7	13.4	7.9	23.0
Rad (W m^{-2})	373	383	211	519	695	720	561	876
Temp. (°C)	6.7	6.9	−0.8	15.1	19.4	20.9	14.5	25.1
RH (%)	58	56	42	74	48	45	34	59

Table 2. The NPF classification and environmental conditions on each chosen case day at SMEAR II and SORPES. Note that condensation sink, meteorological conditions, and the concentrations of trace gases are from 09:00 to 15:00 LT.

Case (MM/DD/YYYY)	NPF classification	CS (10^{-2} s^{-1})	Temp (°C)	Rad (W m^{-2})	RH (%)	O_3 (ppbv)	SO_2 (ppbv)	NO_x (ppbv)	Mono (ppbv)	Benz. (ppbv)
SMEAR II										
05/01/2013	NPF	0.06	7.1	605.1	41.1	36.0	0.03	0.05	0.05	0.08
05/12/2013	Non-NPF	0.3	13.8	553.2	43.0	40.4	0.07	0.08	0.1	0.06
05/16/2013	NPF	0.3	17.6	682.9	27.9	53.2	0.05	0.1	0.2	0.05
05/22/2013	NPF	0.3	16.3	471.7	40.7	35.7	0.2	0.1	0.2	0.06
06/15/2013	NPF	0.1	14.8	486.6	59.0	32.3	0.04	0.07	0.1	0.04
SORPES										
09/22/2014	NPF	2.1	24.6	497.0	60.2	45.2	2.4	7.7	0.04	0.7
09/24/2014	NPF	2.8	25.5	550.5	64.3	44.6	2.5	5.8	0.05	0.4
09/26/2014	Non-NPF	5.5	24.5	298.4	72.5	46.2	5.5	8.8	0.1	0.7
10/04/2014	NPF	2.5	22.2	567.6	53.7	36.2	8.3	22.2	0.04	0.6
10/06/2014	NPF	2.2	20.4	561.4	48.3	41.6	4.1	6.9	0.02	0.3

monomers, dimers, and organonitrates presented in Fig. 2b–d contain 7–14, 8–17, and 7–14 oxygen atoms, respectively. The model predicts the measured diurnal cycle of HOM non-nitrate monomers at SMEAR II with good agreement. For HOM dimers, the simulated concentrations are higher than the measurements at night while they are slightly lower in the daytime when the NPF events occur. For HOM organonitrate, although matching well with measurements in the daytime, the simulation results have a stronger diurnal pattern, with much lower concentrations than measurements at night. In general, the normalized mean bias (NMB) values of sulfuric acid, HOM non-nitrate monomers, dimers, organonitrates, and total HOM are −63.0 %, 11.1 %, 174.3 %, 8.0 %, and 38.3 %, respectively. Considering the uncertainties of the CI-APi-TOF in measuring gas HOMs (estimated uncertainty up to a factor of 2–3) and the many unknowns in their forma-

tions, the model provides an acceptable agreement between simulated and measured vapour concentrations.

Although no measurements of sulfuric acid and HOM are conducted at SORPES, a comparison of the simulated gas vapour concentrations at two sites can help us to qualitatively understand the differences between the boreal forest and polluted areas in China. As shown in Fig. 2a, the simulated sulfuric acid at SORPES is 1 order of magnitude higher than at SMEAR II in the daytime. The high value of sulfuric acid is mainly related to the extremely high SO_2 concentrations and high atmospheric oxidation capacity at SORPES. Such high simulated sulfuric acid concentration is consistent with the measurements conducted in other urban sites in China, e.g. about 10^7 measurements cm^{-3} in Beijing (Z. B. Wang et al., 2013). The simulated HOM non-nitrate monomer concentrations from monoterpene oxidation are lower at SORPES (Fig. 2b) because of low values of monoterpene con-
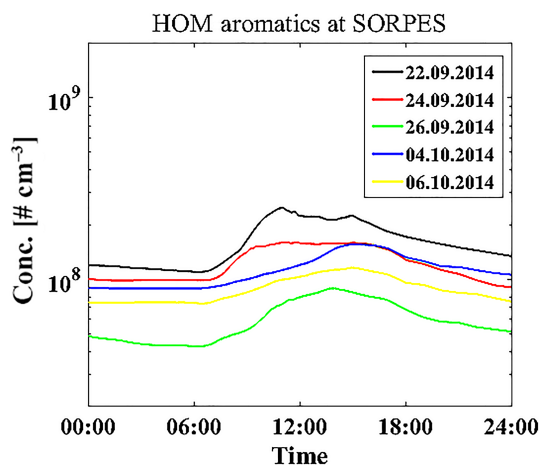
Figure 3. Simulated diurnal cycles of HOMs formed from aromatics oxidation at SORPES on each chosen day.

Table 3. The observed and simulated formation rates of 6 nm particles (J_6) and growth rates of 6–30 nm particles (GR) on chosen NPF days (MM/DD/YYYY) at each site.

	J_6 obs. (cm^{-3} s^{-1})	J_6 sim. (cm^{-3} s^{-2})	GR obs. (nm h^{-1})	GR sim. (nm h^{-1})
SMEAR II				
05/01/2013	0.6	0.3	3.8	3.7
05/16/2013	0.06	0.07	3.3	3.6
05/22/2013	0.05	0.3	4.0	4.5
06/15/2013	0.08	0.6	5.2	4.8
SORPES				
09/22/2014	4.9	5.6	9.9	7.8
09/24/2014	6.9	2.2	16.2	3.3
10/04/2014	3.8	1.8	14.9	2.8
10/06/2014	2.9	0.4	12.9	2.8

3.3 The simulations of aerosol size distributions at two sites

Figure 4 shows the variations in measured and simulated aerosol number size distribution at SMEAR II and SORPES. The kinetic coefficients (k value) on each day at both sites (tuned to cover the observed particle formation rates) is shown in Fig. 4b and d. For the SMEAR II site, the model can capture both the NPF events and non-NPF events with the same k value, i.e. 1×10^{-18} m^3 s^{-1}. Comparing the observed and simulated formation rates of 6 nm particles at SMEAR II (Table 3), the model underestimated the formation rate on 1 May 2013 but overestimated the formation rate on other NPF days. During event days, more than one banana shape was simulated at SMEAR II, which is mainly because of the multi-peaks of simulated sulfuric acid. For the SORPES station, the k value is higher than at SMEAR II on average and with more discrepancies. The k value on 22 September 2014 is more similar to the value at SMEAR II but much lower than on other chosen days. The variations in the k values can reflect the variability in other unaccounted for compounds involved in the particle or cluster formation and initial growth (Kuang et al., 2008). The much higher k values at SORPES except on 22 September 2014 reflect that other compounds, probably oxidation products of anthropogenic pollutants, can also be involved in the nucleation. Moreover, the model cannot simulate the high formation rates observed at SORPES except on 22 September 2014 (Table 3).

For simulations at the SORPES station, the brief formation mechanisms of HOMs from aromatics were added to the MCM and the saturation vapour pressure of HOMs were calculated by SIMPOL. However, even if we decrease the pure liquid saturation vapour pressures of HOMs from aromatics oxidation by 2 orders of magnitude, the model significantly underestimates the growth during the event days, except on 22 September 2014. The simulated growth rates on 22 and
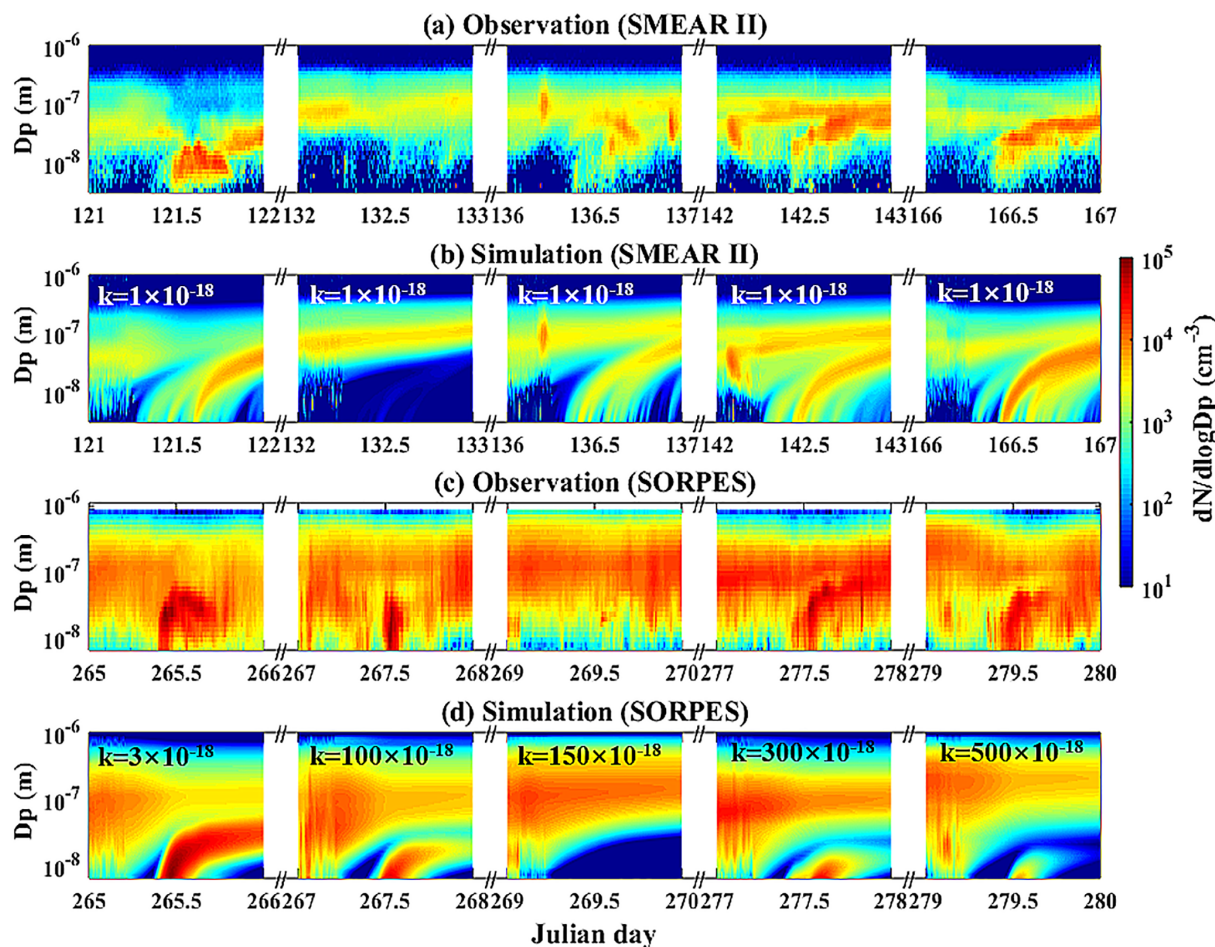
centrations and high condensation sink. The simulated HOM dimer concentrations are much lower at SORPES than at SMEAR II while HOM organonitrate concentrations at SORPES are 1 order of magnitude higher than at SMEAR II (Fig. 2c, d). It is mainly because high NO concentrations at SORPES suppress the HOM dimer formation but contribute to the formation of HOM organonitrates.

The simulated HOM monomer, dimer, and organonitrate concentrations presented in Fig. 2 only refer to the HOMs formed from monoterpene oxidation, which has been believed to be one of the main sources of HOMs and was considered in the MALTE-BOX (Ehn et al., 2014). However, recent lab experiments show that the aromatic hydrocarbons (e.g. benzene, toluene, *o*-/*m*-/*p*-xylene, 1,3,5-/1,2,3-/1,2,4-trimethylbenzene) oxidized by OH can lead to a subsequent autoxidation chain reaction forming HOMs, which is believed to contribute substantially to NPF in urban areas (Molteni et al., 2016). Therefore, according to Molteni et al. (2016), a HOM molar yield of 3 % for the OH oxidation of the aromatic species was assumed and added to MCM v3.3.1. The contributions of aromatics oxidation to the HOMs can be ignored in remote boreal forest because of extremely low aromatics concentrations. However, as shown in Fig. 3, the HOMs from aromatics oxidation at SORPES can be above 10^8 cm^{-3}, which is about 1 order of magnitude higher than HOMs from monoterpene oxidation. HOM concentration from aromatics oxidation on NPF days is obviously higher than non-event days, reflecting an important role of HOMs in NPF. Such a high concentration of HOMs from aromatics oxidation is caused by the high levels of aromatics and OH radicals in the polluted urban environment and may contribute substantially to SOA formation.

Figure 4. (a, c) Measured and **(b, d)** simulated particle number size distribution at SMEAR II and SORPES, respectively. Note the kinetic coefficient on each day is shown in Fig. 4b, d.
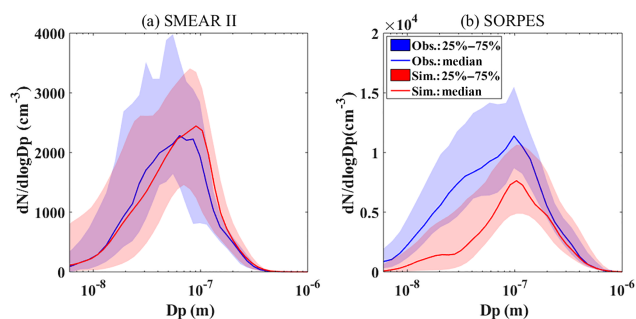

Figure 5. The observed and simulated aerosol number size distributions **(a)** at SMEAR II and **(b)** at SORPES. Note the observed and simulated average (line) and ± 1 SD (shaded area) are in blue and red, respectively.

24 September and 4 and 6 October are 7.8, 3.3, 2.8, and 2.8 nm h^{-1}, compared to the observed growth rates with 9.9, 16.2, 14.9, and 12.9 nm h^{-1}, respectively (Table 3). These results indicate that under polluted environmental conditions

there must be some other important gas vapours that are not accounted for in the model that contributes to the growth. Tao et al. (2016) found that heterogeneous uptake of amines can effectively contribute to particle growth of newly formed particles in the polluted Yangtze River Delta area of China. Heterogeneous uptake of amines has not been included in the MALTE-BOX and might be one of the possible reasons of the underestimation of growth rate. Comparing the observed and simulated number size distribution (Fig. 5), the simulated aerosol size distributions were in good agreement with measurements at SMEAR II, but the simulated number concentrations in the size range below 200 nm at SORPES are extremely lower than the observation. One reason is that primary particle emission is an important source of ultrafine particles in urban areas (Qi et al., 2015), but not accounted for in the model. Another reason is that current chemistry mechanisms and the accounted for VOCs in the model dramatically underestimate SOA formation in polluted areas. In addition to the monoterpene-formed SOA, the MALTE-BOX model also considers the isoprene and anthropogenic SOA.

However, the mechanisms of SOA formation, especially for the anthropogenic SOA, are still unclear and other unconsidered anthropogenic gas vapours in the modelling studies may also contribute to SOA formation.

Only the NPF event on 22 September 2014 was simulated in good agreement with measurements because this day had the lowest condensation sink and highest aromatics concentrations among the chosen NPF cases at SORPES. Figure 6 presents the footprints of all the cases at SORPES. The air mass on 22 September 2014 was from a marine area. A previous study shows that these marine air masses have the lowest accumulation mode particle concentrations and therefore NPF occurs frequently (Qi et al., 2015). Although having the lowest condensation sink, the aromatics concentration on this day was still quite high, which was most probably due to a local petrochemical industrial area. The air masses on 24 September and 6 October were from northern China and brought air pollutants to Nanjing (Fig. 6b, e). On 4 October, the air masses had similar retroplumes to those on 22 September but with more local origin (Fig. 6). Holiday effects in China (national holiday with more family vacations during 1–7 October) caused the high NO_x and anthropogenic VOC concentrations on this day (Xu et al., 2017). The NPF and growth were suppressed by high NO_x concentrations and therefore cannot be simulated by the current MALTE-BOX model.

3.4 The differences of relative contributions of precursor vapours to particle growth at two sites

Figure 7 shows the averaged relative contributions of precursor vapours to the growth of sub-100 nm particles from 09:00 to 15:00 LT during the four chosen NPF days at SMEAR II and on 22 September 2014 at SORPES. Only the NPF event on 22 September 2014 was presented at SORPES because the current MALTE-BOX model can only capture the shape of NPF on this day. At SMEAR II, the growth of ultrafine particles was dominated by HOM from monoterpene oxidation, which is consistent with the previous study by Ehn et al. (2014). HOM monomers contribute most to the growth at SMEAR II as they have high concentrations and relatively low saturation vapour pressures.

The relative contributions of precursor vapours to the growth of particles at SORPES are quite different from those at SMEAR II. First, through the higher gas-phase sulfuric acid concentration at SORPES (as shown in Fig. 2), sulfuric acid has huge contributions to the growth of ultrafine particles at SORPES while playing a minor role in the growth at SMEAR II. Second, high NO concentration at SORPES switches the formation of HOM non-nitrate monomers and dimers to the formation of HOM organonitrates. As under the same oxygen-to-carbon ratio the saturation vapour pressures of organonitrates were higher than non-nitrate monomers and dimers, the HOMs from monoterpene oxidation contribute less to the growth at SORPES in general. Third, at SOR-

PES, HOMs from aromatics oxidation play a dominant role in the growth of ultrafine particles because of high aromatics concentrations. Dai et al. (2017) conducted the simultaneous measurements near a petrochemical industrial area in Nanjing and found that the anthropogenic VOCs have significant contributions to both the nucleation and the growth. This is also consistent with the previous study at SORPES finding that higher growth rates were observed when the air masses were from the Yangtze River Delta area with high anthropogenic VOC emissions (Qi et al., 2015).

4   Conclusions

Higher-frequency formation rates and growth rates of new particle formation (NPF) events were observed at SORPES, a suburban site in eastern China, compared to SMEAR II, a boreal forest site in Finland. To quantitatively understand the differences in NPF at the two sites, the condensing vapours (i.e. sulfuric acid and HOM) and particle number size distributions were simulated by a new version of the MALTE-BOX model with the comprehensive HOM formation mechanism based on monoterpene oxidation and a simplified mechanism of HOM formation from aromatics oxidation.

The model was proven to work well on simulating the sulfuric acid and HOMs from monoterpene oxidation by comparing them with measurements at SMEAR II. Comparing the simulated sulfuric acid and HOMs from monoterpene oxidation at two sites, the sulfuric acid and HOM organonitrate concentrations were much higher while the concentrations of HOM non-nitrate monomers and dimers were lower at SORPES than at SMEAR II. High concentrations of HOMs from aromatics oxidation were simulated at SORPES. The differences in gas vapours (sulfuric acid and HOMs) at two sites are mainly because of the substantially higher SO_2, NO, aromatics concentration, and condensation sink at SORPES. The model can simulate the particle number size distributions on NPF and non-NPF days with same kinetic coefficient at SMEAR II. However, the k value is more divergent at SORPES, which means the mechanism of nucleation in polluted urban areas is more complicated. HOMs from monoterpene oxidation contribute more to the growth at SMEAR II while the sulfuric acid and HOMs from aromatics play dominant roles in the growth of newly formed particles at SORPES. This study highlights that sulfuric acid and HOM concentration and their relative contributions to growth are distinct at different environmental conditions.

In summary, this study gives an example comparing the simulations of NPF and particle growth in different environmental conditions using the MALTE-BOX models with advanced chemical mechanisms. This study demonstrates that the current model has a limited capacity in reproducing NPF and the growth rate in polluted environments like eastern China. To improve the understanding of NPF and SOA formation in the polluted environment, intensive, long-term
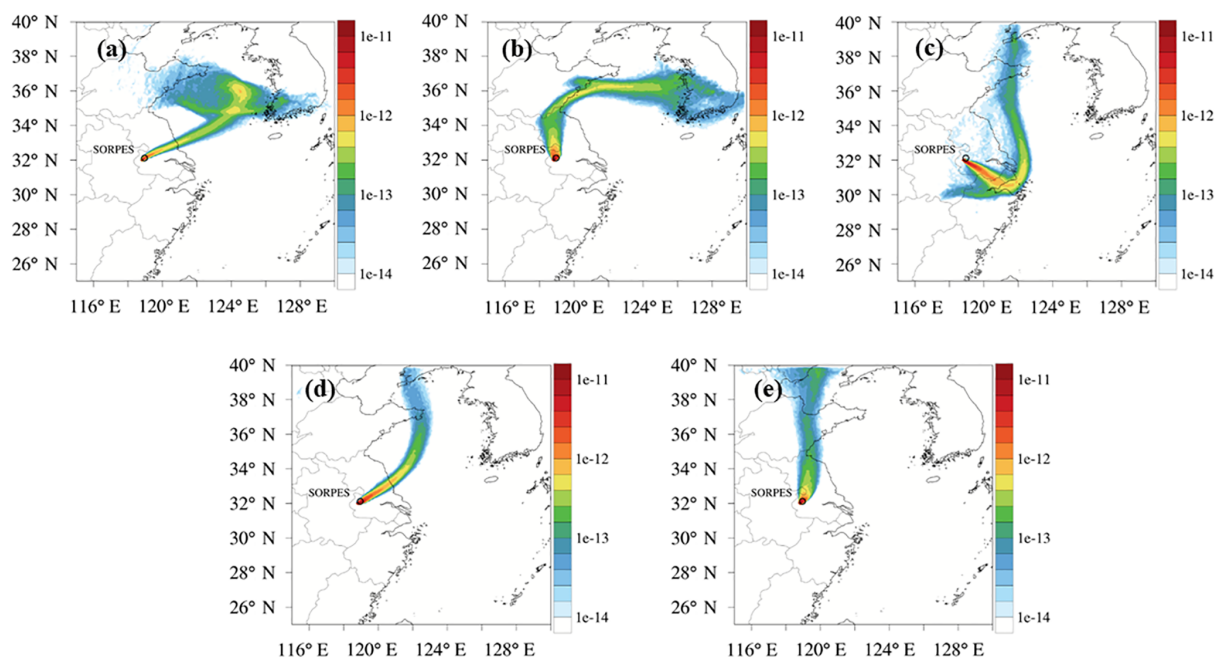
Figure 6. The averaged retroplume (footprint residence time) from 09:00 to 15:00 LT on **(a)** 22 September, **(b)** 24 September, **(c)** 26 September, **(d)** 4 October, and **(e)** 6 October 2014.
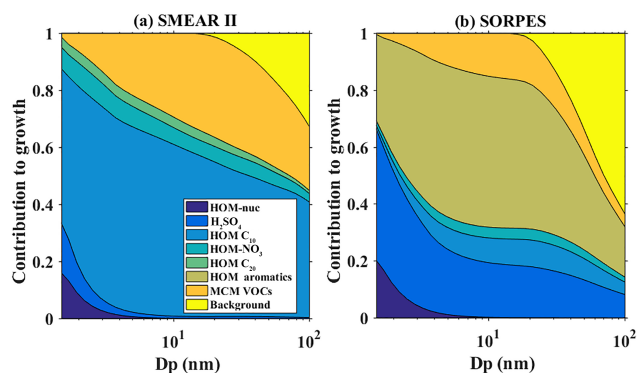

Figure 7. The relative contributions of precursor vapours to the growth of sub-100 nm particles at **(a)** SMEAR II and **(b)** SORPES.

field measurements of HOMs with a CI-APi-TOF, combined with various measurements of gaseous precursors, oxidants, clusters, and aerosol particles are needed in the future. Further developments of the box model based on more quantitative chamber studies are also needed. These efforts will help build a universal chemical mechanism applicable for different (either clean or polluted, anthropogenic or biogenic dominated) environmental conditions in the world and further improve the capability of global air quality and climate models.

Data availability. The data of the SMEAR II station (including meteorological, trace gas, VOCs, aerosol size distribution) are avail-

able at https://avaa.tdata.fi/web/smart (Junninen et al., 2009), and data of SORPES (meteorological, trace gas, VOCs, aerosol size distribution) are available from the corresponding author upon request before the SORPES database is opened publicly. Emission data are available at http://eccad.sedoo.fr/eccad_extract_interface/ (Granier et al., 2011).

The Supplement related to this article is available online at https://doi.org/10.5194/acp-18-11779-2018-supplement.

References

Boy, M., Hellmuth, O., Korhonen, H., Nilsson, E. D., ReVelle, D., Turnipseed, A., Arnold, F., and Kulmala, M.: MALTE-model to predict new aerosol formation in the lower troposphere, Atmos. Chem. Phys., 6, 4499–4517, https://doi.org/10.5194/acp-6-4499-2006, 2006.

Boy, M., Bonn, B., Kazil, J., Lovejoy, N., Turnipseed, A., Greenberg, J., Karl, T., Mauldin, L., Kusciuch, E., Smith, J., Barsanti, K., Guenther, A., Wehner, B., Hellmuth, O., Siebert, H., Bauer, S., Wiedensohler, A., and Kulmala, M.: Relevance of Several Nucleation Theories in Different Environments, in: Nucleation and Atmospheric Aerosols: 17th International Conference, Galway, Ireland, 2007, edited by: O'Dowd, C. D. and Wagner, P. E., Springer Netherlands, Dordrecht, 87–91, 2007.

Boy, M., Kazil, J., Lovejoy, E. R., Guenther, A., and Kulmala, M.: Relevance of ion-induced nucleation of sulfuric acid and water in the lower troposphere over the boreal forest at northern latitudes, Atmos. Res., 90, 151–158, https://doi.org/10.1016/j.atmosres.2008.01.002, 2008.

Boy, M., Mogensen, D., Smolander, S., Zhou, L., Nieminen, T., Paasonen, P., Plass-Dülmer, C., Sipilä, M., Petäjä, T., Mauldin, L., Berresheim, H., and Kulmala, M.: Oxidation of SO_2 by stabilized Criegee intermediate (sCI) radicals as a crucial source for atmospheric sulfuric acid concentrations, Atmos. Chem. Phys., 13, 3865–3879, https://doi.org/10.5194/acp-13-3865-2013, 2013.

Carlton, A. G., Wiedinmyer, C., and Kroll, J. H.: A review of Secondary Organic Aerosol (SOA) formation from isoprene, Atmos. Chem. Phys., 9, 4987–5005, https://doi.org/10.5194/acp-9-4987-2009, 2009.

Dai, L., Wang, H., Zhou, L., An, J., Tang, L., Lu, C., Yan, W., Liu, R., Kong, S., and Chen, M.: Regional and local new particle formation events observed in the Yangtze River Delta region, China, J. Geophys. Res.-Atmos., 122, 2389–2402, 2017.

Dal Maso, M., Kulmala, M., Riipinen, I., Wagner, R., Hussein, T., Aalto, P. P., and Lehtinen, K. E. J.: Formation and growth of fresh atmospheric aerosols: eight years of aerosol size distribution data from SMEAR II, Hyytiala, Finland, Boreal Environ. Res., 10, 323–336, 2005.

Damian, V., Sandu, A., Damian, M., Potra, F., and Carmichael, G. R.: The kinetic preprocessor KPP – a software environment for solving chemical kinetics, Comput. Chem. Eng., 26, 1567–1579, https://doi.org/10.1016/s0098-1354(02)00128-x, 2002.

Ding, A. J., Fu, C. B., Yang, X. Q., Sun, J. N., Zheng, L. F., Xie, Y. N., Herrmann, E., Nie, W., Petäjä, T., Kerminen, V.-M., and Kulmala, M.: Ozone and fine particle in the western Yangtze River Delta: an overview of 1 yr data at the SORPES station, Atmos. Chem. Phys., 13, 5813–5830, https://doi.org/10.5194/acp-13-5813-2013, 2013.

Ding, A. J., Nie, W., Huang, X., Chi, X., Sun, J., Kerminen, V.-M., Xu, Z., Guo, W., Petäjä, T., Yang, X., Kulmala, M., and Fu, C.: Long-term observation of air pollution-weather/climate interactions at the SORPES station: a review and outlook, Front. Environ. Sci. Eng., 10, 15 https://doi.org/10.1007/s11783-016-0877-3, 2016.

Ehn, M., Thornton, J. A., Kleist, E., Sipila, M., Junninen, H., Pullinen, I., Springer, M., Rubach, F., Tillmann, R., Lee, B., Lopez-Hilfiker, F., Andres, S., Acir, I. H., Rissanen, M., Jokinen, T., Schobesberger, S., Kangasluoma, J., Kontkanen, J., Nieminen, T., Kurten, T., Nielsen, L. B., Jorgensen, S., Kjaergaard, H. G., Canagaratna, M., Dal Maso, M., Berndt, T., Petäjä, T., Wahner, A., Kerminen, V. M., Kulmala, M., Worsnop, D. R., Wildt, J., and Mentel, T. F.: A large source of low-volatility secondary organic aerosol, Nature, 506, 476–479, https://doi.org/10.1038/nature13032, 2014.

Granier, C., Bessagnet, B., Bond, T., D'Angiola, A., van der Gon, H. D., Frost, G. J., Heil, A., Kaiser, J. W., Kinne, S., Klimont, Z., Kloster, S., Lamarque, J. F., Liousse, C., Masui, T., Meleux, F., Mieville, A., Ohara, T., Raut, J. C., Riahi, K., Schultz, M. G., Smith, S. J., Thompson, A., van Aardenne, J., van der Werf, G. R., and van Vuuren, D. P.: Evolution of anthropogenic and biomass burning emissions of air pollutants at global and regional scales during the 1980–2010 period, Clim. Change, 109, 163–190, https://doi.org/10.1007/s10584-011-0154-1, 2011.

Guo, S., Hu, M., Zamora, M. L., Peng, J. F., Shang, D. J., Zheng, J., Du, Z. F., Wu, Z., Shao, M., Zeng, L. M., Molina, M. J., and Zhang, R. Y.: Elucidating severe urban haze formation in China, P. Natl. Acad. Sci. USA, 111, 17373–17378, https://doi.org/10.1073/pnas.1419604111, 2014.

Hakola, H., Hellén, H., Hemmilä, M., Rinne, J., and Kulmala, M.: In situ measurements of volatile organic compounds in a boreal forest, Atmos. Chem. Phys., 12, 11665–11678, https://doi.org/10.5194/acp-12-11665-2012, 2012.

Hari, P., Nikinmaa, E., Pohja, T., Siivola, E., Bäck, J., Vesala, T., and Kulmala, M.: Station for Measuring Ecosystem-Atmosphere Relations: SMEAR, in: Physical and Physiological Forest Ecology, edited by: Hari, P., Heliövaara, K., and Kulmala, L., Springer Netherlands, Dordrecht, 471–487, 2013.

Hu, J., Wang, P., Ying, Q., Zhang, H., Chen, J., Ge, X., Li, X., Jiang, J., Wang, S., Zhang, J., Zhao, Y., and Zhang, Y.: Modeling biogenic and anthropogenic secondary organic aerosol in China, Atmos. Chem. Phys., 17, 77–92, https://doi.org/10.5194/acp-17-77-2017, 2017.

Huang, X., Zhou, L., Ding, A., Qi, X., Nie, W., Wang, M., Chi, X., Petäjä, T., Kerminen, V.-M., Roldin, P., Rusanen, A., Kulmala, M., and Boy, M.: Comprehensive modelling study on observed new particle formation at the SORPES sta-

tion in Nanjing, China, Atmos. Chem. Phys., 16, 2477–2492, https://doi.org/10.5194/acp-16-2477-2016, 2016.

Jenkin, M. E., Saunders, S. M., Wagner, V., and Pilling, M. J.: Protocol for the development of the Master Chemical Mechanism, MCM v3 (Part B): tropospheric degradation of aromatic volatile organic compounds, Atmos. Chem. Phys., 3, 181–193, https://doi.org/10.5194/acp-3-181-2003, 2003.

Jokinen, T., Berndt, T., Makkonen, R., Kerminen, V. M., Junninen, H., Paasonen, P., Stratmann, F., Herrmann, H., Guenther, A. B., Worsnop, D. R., Kulmala, M., Ehn, M., and Sipila, M.: Production of extremely low volatile organic compounds from biogenic emissions: Measured yields and atmospheric implications, P. Natl. Acad. Sci. USA, 112, 7123–7128, 10.1073/pnas.1423977112, 2015.

Junninen, H., Lauri, A., Keronen, P., Aalto, P., Hiltunen, V., Hari, P., and Kulmala, M.: SMART-SMEAR: on-line data exploration and visualization tool for SMEAR stations, Boreal Environ. Res., 14, 447–457, 2009.

Kivekas, N., Sun, J., Zhan, M., Kerminen, V. M., Hyvarinen, A., Komppula, M., Viisanen, Y., Hong, N., Zhang, Y., Kulmala, M., Zhang, X. C., Deli, G., and Lihavainen, H.: Long term particle size distribution measurements at Mount Waliguan, a high-altitude site in inland China, Atmos. Chem. Phys., 9, 5461–5474, 2009.

Korhonen, H., Lehtinen, K. E. J., and Kulmala, M.: Multi-component aerosol dynamics model UHMA: model development and validation, Atmos. Chem. Phys., 4, 757–771, https://doi.org/10.5194/acp-4-757-2004, 2004.

Kuang, C., McMurry, P. H., McCormick, A. V., and Eisele, F. L.: Dependence of nucleation rates on sulfuric acid vapor concentration in diverse atmospheric locations, J. Geophys. Res.-Atmos., 113, D10209, https://doi.org/10.1029/2007jd009253, 2008.

Kulmala, M., Vehkamaki, H., Petaja, T., Dal Maso, M., Lauri, A., Kerminen, V. M., Birmili, W., and McMurry, P. H.: Formation and growth rates of ultrafine atmospheric particles: a review of observations, J. Aerosol Sci., 35, 143–176, https://doi.org/10.1016/j.jaerosci.2003.10.003, 2004.

Kulmala, M. and Kerminen, V. M.: On the formation and growth of atmospheric nanoparticles, Atmos. Res., 90, 132–150, https://doi.org/10.1016/j.atmosres.2008.01.005, 2008.

Kulmala, M., Kontkanen, J., Junninen, H., Lehtipalo, K., Manninen, H. E., Nieminen, T., Petaja, T., Sipila, M., Schobesberger, S., Rantala, P., Franchin, A., Jokinen, T., Jarvinen, E., Aijala, M., Kangasluoma, J., Hakala, J., Aalto, P. P., Paasonen, P., Mikkila, J., Vanhanen, J., Aalto, J., Hakola, H., Makkonen, U., Ruuskanen, T., Mauldin, R. L., Duplissy, J., Vehkamaki, H., Back, J., Kortelainen, A., Riipinen, I., Kurten, T., Johnston, M. V., Smith, J. N., Ehn, M., Mentel, T. F., Lehtinen, K. E. J., Laaksonen, A., Kerminen, V. M., and Worsnop, D. R.: Direct Observations of Atmospheric Aerosol Nucleation, Science, 339, 943–946, https://doi.org/10.1126/science.1227385, 2013.

Kulmala, M., Petaja, T., Ehn, M., Thornton, J., Sipila, M., Worsnop, D. R., and Kerminen, V. M.: Chemistry of Atmospheric Nucleation: On the Recent Advances on Precursor Characterization and Atmospheric Cluster Composition in Connection with Atmospheric New Particle Formation, Annu. Rev. Phys. Chem., 65, 21–37, https://doi.org/10.1146/annurev-physchem-040412-110014, 2014.

Kulmala, M., Lappalainen, H. K., Petäjä, T., Kurten, T., Kerminen, V.-M., Viisanen, Y., Hari, P., Sorvari, S., Bäck, J., Bondur, V., Kasimov, N., Kotlyakov, V., Matvienko, G., Baklanov, A., Guo, H. D., Ding, A., Hansson, H.-C., and Zilitinkevich, S.: Introduction: The Pan-Eurasian Experiment (PEEX) – multidisciplinary, multiscale and multicomponent research and capacity-building initiative, Atmos. Chem. Phys., 15, 13085–13096, https://doi.org/10.5194/acp-15-13085-2015, 2015.

Kulmala, M., Kerminen, V. M., Petaja, T., Ding, A. J., and Wang, L.: Atmospheric gas-to-particle conversion: why NPF events are observed in megacities?, Faraday Discuss., 200, 271–288, https://doi.org/10.1039/c6fd00257a, 2017.

Kurteìn, T., Tiusanen, K., Roldin, P., Rissanen, M., Luy, J.-N., Boy, M., Ehn, M., and Donahue, N.: α-Pinene autoxidation products may not have extremely low saturation vapor pressures despite high O : C ratios, J. Phys. Chem. A, 120, 2569–2582, 2016.

Lappalainen, H. K., Kerminen, V.-M., Petäjä, T., Kurten, T., Baklanov, A., Shvidenko, A., Bäck, J., Vihma, T., Alekseychik, P., Andreae, M. O., Arnold, S. R., Arshinov, M., Asmi, E., Belan, B., Bobylev, L., Chalov, S., Cheng, Y., Chubarova, N., de Leeuw, G., Ding, A., Dobrolyubov, S., Dubtsov, S., Dyukarev, E., Elansky, N., Eleftheriadis, K., Esau, I., Filatov, N., Flint, M., Fu, C., Glezer, O., Gliko, A., Heimann, M., Holtslag, A. A. M., Hõrrak, U., Janhunen, J., Juhola, S., Järvi, L., Järvinen, H., Kanukhina, A., Konstantinov, P., Kotlyakov, V., Kieloaho, A.-J., Komarov, A. S., Kujansuu, J., Kukkonen, I., Duplissy, E.-M., Laaksonen, A., Laurila, T., Lihavainen, H., Lisitzin, A., Mahura, A., Makshtas, A., Mareev, E., Mazon, S., Matishov, D., Melnikov, V., Mikhailov, E., Moisseev, D., Nigmatulin, R., Noe, S. M., Ojala, A., Pihlatie, M., Popovicheva, O., Pumpanen, J., Regerand, T., Repina, I., Shcherbinin, A., Shevchenko, V., Sipilä, M., Skorokhod, A., Spracklen, D. V., Su, H., Subetto, D. A., Sun, J., Terzhevik, A. Y., Timofeyev, Y., Troitskaya, Y., Tynkkynen, V.-P., Kharuk, V. I., Zaytseva, N., Zhang, J., Viisanen, Y., Vesala, T., Hari, P., Hansson, H. C., Matvienko, G. G., Kasimov, N. S., Guo, H., Bondur, V., Zilitinkevich, S., and Kulmala, M.: Pan-Eurasian Experiment (PEEX): towards a holistic understanding of the feedbacks and interactions in the land-atmosphere-ocean-society continuum in the northern Eurasian region, Atmos. Chem. Phys., 16, 14421–14461, https://doi.org/10.5194/acp-16-14421-2016, 2016.

Merikanto, J., Spracklen, D. V., Mann, G. W., Pickering, S. J., and Carslaw, K. S.: Impact of nucleation on global CCN, Atmos. Chem. Phys., 9, 8601–8616, https://doi.org/10.5194/acp-9-8601-2009, 2009.

Molteni, U., Bianchi, F., Klein, F., El Haddad, I., Frege, C., Rossi, M. J., Dommen, J., and Baltensperger, U.: Formation of highly oxygenated organic molecules from aromatic compounds, Atmos. Chem. Phys., 18, 1909–1921, https://doi.org/10.5194/acp-18-1909-2018, 2018.

Nan, J., Wang, S., Guo, Y., Xiang, Y., and Zhou, B.: Study on the daytime OH radical and implication for its relationship with fine particles over megacity of Shanghai, China, Atmos. Environ., 154, 167–178, 2017.

Nannoolal, Y., Rarey, J., and Ramjugernath, D.: Estimation of pure component properties: Part 3. Estimation of the vapor pressure of non-electrolyte organic compounds via group contributions and group interactions, Fluid Phase Equilibr., 269, 117–133, 2008.

Nieminen, T., Asmi, A., Dal Maso, M., Aalto, P. P., Keronen, P., Petäjä, T., Kulmala, M., and Kerminen, V.-M.: Trends in atmospheric new-particle formation: 16 years of observations in a boreal-forest environment, Boreal Environ. Res., 19, 191–214, 2014.

Ortega, I. K., Suni, T., Boy, M., Grönholm, T., Manninen, H. E., Nieminen, T., Ehn, M., Junninen, H., Hakola, H., Hellén, H., Valmari, T., Arvela, H., Zegelin, S., Hughes, D., Kitchen, M., Cleugh, H., Worsnop, D. R., Kulmala, M., and Kerminen, V.-M.: New insights into nocturnal nucleation, Atmos. Chem. Phys., 12, 4297–4312, https://doi.org/10.5194/acp-12-4297-2012, 2012.

Öström, E., Putian, Z., Schurgers, G., Mishurov, M., Kivekäs, N., Lihavainen, H., Ehn, M., Rissanen, M. P., Kurtén, T., Boy, M., Swietlicki, E., and Roldin, P.: Modeling the role of highly oxidized multifunctional organic molecules for the growth of new particles over the boreal forest region, Atmos. Chem. Phys., 17, 8887–8901, https://doi.org/10.5194/acp-17-8887-2017, 2017.

Pankow, J. F. and Asher, W. E.: SIMPOL.1: a simple group contribution method for predicting vapor pressures and enthalpies of vaporization of multifunctional organic compounds, Atmos. Chem. Phys., 8, 2773–2796, https://doi.org/10.5194/acp-8-2773-2008, 2008.

Petäjä, T., Mauldin III, R. L., Kosciuch, E., McGrath, J., Nieminen, T., Paasonen, P., Boy, M., Adamov, A., Kotiaho, T., and Kulmala, M.: Sulfuric acid and OH concentrations in a boreal forest site, Atmos. Chem. Phys., 9, 7435–7448, https://doi.org/10.5194/acp-9-7435-2009, 2009.

Qi, X. M., Ding, A. J., Nie, W., Petäjä, T., Kerminen, V.-M., Herrmann, E., Xie, Y. N., Zheng, L. F., Manninen, H., Aalto, P., Sun, J. N., Xu, Z. N., Chi, X. G., Huang, X., Boy, M., Virkkula, A., Yang, X.-Q., Fu, C. B., and Kulmala, M.: Aerosol size distribution and new particle formation in the western Yangtze River Delta of China: 2 years of measurements at the SORPES station, Atmos. Chem. Phys., 15, 12445–12464, https://doi.org/10.5194/acp-15-12445-2015, 2015.

Riccobono, F., Schobesberger, S., Scott, C. E., Dommen, J., Ortega, I. K., Rondo, L., Almeida, J., Amorim, A., Bianchi, F., Breitenlechner, M., David, A., Downard, A., Dunne, E. M., Duplissy, J., Ehrhart, S., Flagan, R. C., Franchin, A., Hansel, A., Junninen, H., Kajos, M., Keskinen, H., Kupc, A., Kurten, A., Kvashin, A. N., Laaksonen, A., Lehtipalo, K., Makhmutov, V., Mathot, S., Nieminen, T., Onnela, A., Petaja, T., Praplan, A. P., Santos, F. D., Schallhart, S., Seinfeld, J. H., Sipila, M., Spracklen, D. V., Stozhkov, Y., Stratmann, F., Tome, A., Tsagkogeorgas, G., Vaattovaara, P., Viisanen, Y., Vrtala, A., Wagner, P. E., Weingartner, E., Wex, H., Wimmer, D., Carslaw, K. S., Curtius, J., Donahue, N. M., Kirkby, J., Kulmala, M., Worsnop, D. R., and Baltensperger, U.: Oxidation Products of Biogenic Emissions Contribute to Nucleation of Atmospheric Particles, Science, 344, 717–721, https://doi.org/10.1126/science.1243527, 2014.

Roldin, P., Liao, L., Mogensen, D., Dal Maso, M., Rusanen, A., Kerminen, V.-M., Mentel, T. F., Wildt, J., Kleist, E., Kiendler-Scharr, A., Tillmann, R., Ehn, M., Kulmala, M., and Boy, M.: Modelling the contribution of biogenic volatile organic compounds to new particle formation in the Jülich plant atmosphere chamber, Atmos. Chem. Phys., 15, 10777–10798, https://doi.org/10.5194/acp-15-10777-2015, 2015.

Saunders, S. M., Jenkin, M. E., Derwent, R. G., and Pilling, M. J.: Protocol for the development of the Master Chemical Mechanism, MCM v3 (Part A): tropospheric degradation of non-aromatic volatile organic compounds, Atmos. Chem. Phys., 3, 161–180, https://doi.org/10.5194/acp-3-161-2003, 2003.

Schobesberger, S., Junninen, H., Bianchi, F., Lonn, G., Ehn, M., Lehtipalo, K., Dommen, J., Ehrhart, S., Ortega, I. K., Franchin, A., Nieminen, T., Riccobono, F., Hutterli, M., Duplissy, J., Almeida, J., Amorim, A., Breitenlechner, M., Downard, A. J., Dunne, E. M., Flagan, R. C., Kajos, M., Keskinen, H., Kirkby, J., Kupc, A., Kurten, A., Kurten, T., Laaksonen, A., Mathot, S., Onnela, A., Praplan, A. P., Rondo, L., Santos, F. D., Schallhart, S., Schnitzhofer, R., Sipila, M., Tome, A., Tsagkogeorgas, G., Vehkamaki, H., Wimmer, D., Baltensperger, U., Carslaw, K. S., Curtius, J., Hansel, A., Petaja, T., Kulmala, M., Donahue, N. M., and Worsnop, D. R.: Molecular understanding of atmospheric particle formation from sulfuric acid and large oxidized organic molecules, P. Natl. Acad. Sci. USA, 110, 17223–17228, https://doi.org/10.1073/pnas.1306973110, 2013.

Shen, X. J., Sun, J. Y., Zhang, Y. M., Wehner, B., Nowak, A., Tuch, T., Zhang, X. C., Wang, T. T., Zhou, H. G., Zhang, X. L., Dong, F., Birmili, W., and Wiedensohler, A.: First long-term study of particle number size distributions and new particle formation events of regional aerosol in the North China Plain, Atmos. Chem. Phys., 11, 1565–1580, https://doi.org/10.5194/acp-11-1565-2011, 2011.

Sihto, S.-L., Mikkilä, J., Vanhanen, J., Ehn, M., Liao, L., Lehtipalo, K., Aalto, P. P., Duplissy, J., Petäjä, T., Kerminen, V.-M., Boy, M., and Kulmala, M.: Seasonal variation of CCN concentrations and aerosol activation properties in boreal forest, Atmos. Chem. Phys., 11, 13269–13285, https://doi.org/10.5194/acp-11-13269-2011, 2011.

Sindelarova, K., Granier, C., Bouarar, I., Guenther, A., Tilmes, S., Stavrakou, T., Müller, J.-F., Kuhn, U., Stefani, P., and Knorr, W.: Global data set of biogenic VOC emissions calculated by the MEGAN model over the last 30 years, Atmos. Chem. Phys., 14, 9317–9341, https://doi.org/10.5194/acp-14-9317-2014, 2014.

Tao, Y., Ye, X., Jiang, S., Yang, X., Chen, J., Xie, Y., and Wang, R.: Effects of amines on particle growth observed in new particle formation events, J. Geophys. Res.-Atmos., 121, 324–335, 2016.

Topping, D., Barley, M., Bane, M. K., Higham, N., Aumont, B., Dingle, N., and McFiggans, G.: UManSysProp v1.0: an online and open-source facility for molecular property prediction and atmospheric aerosol calculations, Geosci. Model Dev., 9, 899–914, https://doi.org/10.5194/gmd-9-899-2016, 2016.

Trostl, J., Chuang, W. K., Gordon, H., Heinritzi, M., Yan, C., Molteni, U., Ahlm, L., Frege, C., Bianchi, F., Wagner, R., Simon, M., Lehtipalo, K., Williamson, C., Craven, J. S., Duplissy, J., Adamov, A., Almeida, J., Bernhammer, A. K., Breitenlechner, M., Brilke, S., Dias, A., Ehrhart, S., Flagan, R. C., Franchin, A., Fuchs, C., Guida, R., Gysel, M., Hansel, A., Hoyle, C. R., Jokinen, T., Junninen, H., Kangasluoma, J., Keskinen, H., Kim, J., Krapf, M., Kurten, A., Laaksonen, A., Lawler, M., Leiminger, M., Mathot, S., Mohler, O., Nieminen, T., Onnela, A., Petaja, T., Piel, F. M., Miettinen, P., Rissanen, M. P., Rondo, L., Sarnela, N., Schobesberger, S., Sengupta, K., Sipila, M., Smith, J. N., Steiner, G., Tome, A., Virtanen, A., Wagner, A. C., Weingartner, E., Wimmer, D., Winkler, P. M., Ye, P. L., Carslaw, K. S., Curtius, J., Dommen, J., Kirkby, J., Kulmala, M., Riipinen, I., Worsnop, D. R., Donahue, N. M., and Baltensperger, U.: The role of low-volatility organic compounds in

initial particle growth in the atmosphere, Nature, 533, 527–531, https://doi.org/10.1038/nature18271, 2016.

Tsagkogeorgas, G., Roldin, P., Duplissy, J., Rondo, L., Tröstl, J., Slowik, J. G., Ehrhart, S., Franchin, A., Kürten, A., Amorim, A., Bianchi, F., Kirkby, J., Petäjä, T., Baltensperger, U., Boy, M., Curtius, J., Flagan, R. C., Kulmala, M., Donahue, N. M., and Stratmann, F.: Evaporation of sulfate aerosols at low relative humidity, Atmos. Chem. Phys., 17, 8923–8938, https://doi.org/10.5194/acp-17-8923-2017, 2017.

Wang, S., Shi, C., Zhou, B., Zhao, H., Wang, Z., Yang, S., and Chen, L.: Observation of NO$_3$ radicals over Shanghai, China, Atmos. Environ., 70, 401–409, 2013.

Wang, Z. B., Hu, M., Mogensen, D., Yue, D. L., Zheng, J., Zhang, R. Y., Liu, Y., Yuan, B., Li, X., Shao, M., Zhou, L., Wu, Z. J., Wiedensohler, A., and Boy, M.: The simulations of sulfuric acid concentration and new particle formation in an urban atmosphere in China, Atmos. Chem. Phys., 13, 11157–11167, https://doi.org/10.5194/acp-13-11157-2013, 2013.

Wang, Z. B., Wu, Z., Yue, D., Shang, D., Guo, S., Sun, J., Ding, A., Wang, L., Jiang, J., Guo, H., Gao, J., Cheung, H. C., Morawska, L., Keywood, M., and Hu, M.: New particle formation in China: Current knowledge and further directions, Sci. Tot. Environ., 577, 258–266, https://doi.org/10.1016/j.scitotenv.2016.10.177, 2017.

Wildt, J., Mentel, T. F., Kiendler-Scharr, A., Hoffmann, T., Andres, S., Ehn, M., Kleist, E., Müsgen, P., Rohrer, F., Rudich, Y., Springer, M., Tillmann, R., and Wahner, A.: Suppression of new particle formation from monoterpene oxidation by NO$_x$, Atmos. Chem. Phys., 14, 2789–2804, https://doi.org/10.5194/acp-14-2789-2014, 2014.

Wu, Z. J., Hu, M., Liu, S., Wehner, B., Bauer, S., Ssling, A. M., Wiedensohler, A., Petaja, T., Dal Maso, M., and Kulmala, M.: New particle formation in Beijing, China: Statistical analysis of a 1-year data set, J. Geophys. Res.-Atmos., 112, D09209, https://doi.org/10.1029/2006jd007406, 2007.

Xu, Z., Huang, X., Nie, W., Chi, X., Xu, Z., Zheng, L., Sun, P., and Ding, A.: Influence of synoptic condition and holiday effects on VOCs and ozone production in the Yangtze River Delta region, China, Atmos. Environ., 168, 112–124, https://doi.org/10.1016/j.atmosenv.2017.08.035, 2017.

Yan, C., Nie, W., Äijälä, M., Rissanen, M. P., Canagaratna, M. R., Massoli, P., Junninen, H., Jokinen, T., Sarnela, N., Häme, S. A. K., Schobesberger, S., Canonaco, F., Yao, L., Prévôt, A. S. H., Petäjä, T., Kulmala, M., Sipilä, M., Worsnop, D. R., and Ehn, M.: Source characterization of highly oxidized multifunctional compounds in a boreal forest environment using positive matrix factorization, Atmos. Chem. Phys., 16, 12715–12731, https://doi.org/10.5194/acp-16-12715-2016, 2016.

Yu, F. Q., Luo, G., Bates, T. S., Anderson, B., Clarke, A., Kapustin, V., Yantosca, R. M., Wang, Y. X., and Wu, S. L.: Spatial distributions of particle number concentrations in the global troposphere: Simulations, observations, and implications for nucleation mechanisms, J. Geophys. Res.-Atmos., 115, D17205, https://doi.org/10.1029/2009jd013473, 2010.

Zhang, R. Y., Khalizov, A., Wang, L., Hu, M., and Xu, W.: Nucleation and Growth of Nanoparticles in the Atmosphere, Chem. Rev., 112, 1957–2011, https://doi.org/10.1021/cr2001756, 2012.

Zhang, Y., Ding, A., Mao, H., Nie, W., Zhou, D., Liu, L., Huang, X. and Fu, C.: Impact of synoptic weather patterns and inter-decadal climate variability on air quality in the North China Plain during 1980–2013, Atmos. Environ., 124, 119–128, 2016.

Zhang, Y. J., Tang, L. L., Sun, Y. L., Favez, O., Canonaco, F., Albinet, A., Couvidat, F., Liu, D. T., Jayne, J. T., Wang, Z., Croteau, P. L., Canagaratna, M. R., Zhou, H. C., Prevot, A. S. H., and Worsnop, D. R.: Limited formation of isoprene epoxydiols-derived secondary organic aerosol under NO$_x$-rich environments in Eastern China, Geophys. Res. Lett., 44, 2035–2043, 10.1002/2016gl072368, 2017.

Zhou, L. X., Nieminen, T., Mogensen, D., Smolander, S., Rusanen, A., Kulmala, M., and Boy, M.: SOSAA – a new model to simulate the concentrations of organic vapours, sulphuric acid and aerosols inside the ABL – Part 2: Aerosol dynamics and one case study at a boreal forest site, Boreal Environ. Res., 19, 237–256, 2014.